

AperTO - Archivio Istituzionale Open Access dell'Università di Torino

## Mechanistic Insights on the Photosensitized Chemistry of a Fatty Acid at the Air/Water Interface

### This is the author's manuscript

*Original Citation:*

*Availability:*

This version is available <http://hdl.handle.net/2318/1700790> since 2019-05-04T11:46:22Z

*Published version:*

DOI:10.1021/acs.est.6b03165

*Terms of use:*

Open Access

Anyone can freely access the full text of works made available as "Open Access". Works made available under a Creative Commons license can be used according to the terms and conditions of said license. Use of all other works requires consent of the right holder (author or publisher) if not exempted from copyright protection by the applicable law.

(Article begins on next page)

# Mechanistic insights on the photosensitized chemistry of a fatty acid at the air/water interface

*Liselotte Tinel,<sup>#,†,£</sup> Stéphanie Rossignol,<sup>#,†</sup> Angelica Bianco,<sup>‡</sup> Monica Passananti,<sup>†</sup> Sébastien  
Perrier,<sup>†</sup> Xinming Wang,<sup>§</sup> Marcello Brigante,<sup>‡</sup> D. James Donaldson,<sup>¥</sup> Christian George,<sup>\*,†,£</sup>*

*<sup>†</sup> Université Lyon 1, CNRS, UMR 5256, IRCELYON, Institut de recherches sur la catalyse et  
l'environnement de Lyon, 2 avenue Albert Einstein, F-69626 Villeurbanne, France*

*<sup>‡</sup> Université Clermont Auvergne, Université Blaise Pascal, Institut de Chimie de Clermont-  
Ferrand, BP 10448, F-63000 Clermont-Ferrand, FRANCE*

*<sup>§</sup> State Key Laboratory of Organic Geochemistry, Guangzhou Institute of Geochemistry, Chinese  
Academy of Sciences, Guangzhou 510640, China*

*<sup>¥</sup> Department of Chemistry, University of Toronto, 80 St. George St. Toronto, ON Canada M5S  
3H6*

*<sup>£</sup>: Currently at the Wolfson Atmospheric Chemistry Laboratories, Department of Chemistry,  
University of York, YO10 5DD, UK.*

KEYWORDS Photochemical reactions, surface microlayer, air/sea interface, photosensitized  
reactions, 4-benzoyl-benzoic acid, nonanoic acid

Formatted: English (United States)

Formatted: Superscript

18  
19 Interfaces are ubiquitous in the environment and many atmospheric key processes, such as gas  
20 deposition, aerosol and cloud formation are, at one stage or another, strongly impacted by  
21 physical and chemical processes occurring at interfaces. Here, the photo-induced chemistry of an  
22 air/water interface coated with nonanoic acid - a fatty acid surfactant we use as a proxy for  
23 chemically complex natural aqueous surface microlayers - was investigated as a source of  
24 volatile and semi-volatile reactive organic species. The carboxylic acid coating significantly  
25 increased the propensity of photosensitizers, chosen to mimic those observed in real  
26 environmental waters, to partition to the interface and enhance reactivity there. Photochemical  
27 formation of functionalized and unsaturated compounds was systematically observed upon  
28 irradiation of these coated surfaces. The role of a coated interface appears to be critical in  
29 providing a concentrated medium allowing radical-radical reactions to occur in parallel with  
30 molecular oxygen additions. Mechanistic insights are provided from extensive analysis of  
31 products observed in both gas and aqueous phases by on-line SRI-ToF-MS and off-line  
32 UPLC/(±)HESI-HRMS, respectively.

33

## 34 **Introduction**

35 The air/water interface is perhaps the most widespread surface in Earth's environment. Cloud  
36 droplets, lakes, seas and oceans all exhibit very large surfaces that play a crucial role in the  
37 exchange of matter between the hydrosphere and the atmosphere. The understanding of the  
38 specific processes occurring at such interfaces is thus of importance from an atmospheric point  
39 of view. Environmental air/water interfaces often show the presence of surfactants, which are

known to impact the physical processes there. For instance, the transfer between the aqueous phase and the gas phase is restrained in the presence of an insoluble organic coating, which is able to inhibit both water evaporation and solubilization of trace gases.<sup>1</sup> Moreover, organic coated air/water interfaces are expected to increase the surface concentrations of a variety of hydrophobic compounds, possibly impacting their phase transfers.<sup>1</sup> These coated interfaces can also play a role in the removal of atmospheric gases. For example, dry deposition on organic coated water surfaces is suspected to constitute an important sink for ozone in the marine boundary layer, both through its reactivity with the components of the coating material and through increased solubility in this thin organic layer.<sup>1, 2</sup> These air/water surfaces are furthermore exposed to solar light for much of the time and specific photochemical processes are therefore expected to occur there.<sup>3, 4</sup> One interface of particular interest is the sea Surface MicroLayer (sea-SML), defined as the uppermost 1  $\mu\text{m}$  to 1 mm of the surface of the ocean, which is mainly composed of biogenic organics species such as lipids, hydrocarbons, proteins or polysaccharides. It was shown that light absorbing compounds, such as the natural Chromophoric Dissolved Organic Matter (CDOM), are more concentrated in the sea-SML than in the bulk water<sup>5, 6</sup> and therefore it has been speculated that photosensitized reactions could be particularly important in this region, although these processes are still poorly understood and neglected in atmospheric models.<sup>3, 7, 8</sup> Contrary to what was previously thought, the SML is widespread over the sea surface and stable under wind speeds up to 6.6 m s<sup>-1</sup>.<sup>9</sup> Evidence also shows rapid reformation, within minutes, of the perturbed SML.<sup>10</sup> In direct contact with the atmosphere, the role the SML plays in the physical and chemical regulation of emission and uptake of volatile organic compounds (VOCs) and trace gases is still to be clarified.<sup>11</sup> Light absorbing species within the SML can participate in heterogeneous light-induced or light-enhanced reactions with trace gases

at the interface, as has been shown for NO<sub>2</sub> reacting with humic acids or for ozone with chlorophyll.<sup>12, 13</sup> These photochemical reactions can also be a source of gaseous reactive species, as demonstrated for the light induced release of volatile halogen radicals above organic films.<sup>14</sup> <sup>15</sup> In another context, the SML sampled in a commercial rice field, highly enriched in pesticides with concentrations up to 10<sup>5</sup> times higher than in the subsurface waters, showed an enhanced degradation for the pesticide thiobencarb compared to the sampled subsurface water.<sup>16</sup> Organic coatings can thus have significant impacts on the interfacial processes compared to pure water surfaces, particularly if photosensitizers show a propensity to partition to this organic layer.

Recently, spectrometric measurements of the gas phase above an irradiated real sea-SML sample or synthetic nonanoic acid SML enriched with humic acids, showed the formation of a wide variety of functionalized VOCs.<sup>17, 18</sup> The photosensitized formation of unsaturated compounds from a synthetic 1-octanol interfacial layer was also evidenced.<sup>19</sup> These surface photochemical pathways could constitute a still unaccounted for abiotic source of VOCs in the marine boundary layer and in all atmospheric environments where large air/water interfaces are present. In particular the fate of common organic acids, who are relatively unreactive in the gas-phase,<sup>20</sup> could present an ubiquitous photochemical substrate and a source of VOCs in the SML, where such photochemical reactions would compete with *e.g.* oxidation by hydroxyl radicals. Nevertheless, the chemical formation routes of these VOCs are still poorly understood as well as the role of the organic coating on the concentration of photosensitizers at the interface.

This work presents the study of photochemical reactions in a synthetic SML, composed of a saturated carboxylic acid, nonanoic acid (NA), in the presence of known photosensitizers (4-benzoylbenzoic acid and imidazole-2-carboxaldehyde). It focuses on the fundamental processes leading to the formation of functionalized and unsaturated compounds in the gas and condensed

Formatted: Font: Italic

Formatted: Font: Italic

bulk phases. UV-vis spectroscopy and surface fluorescence experiments were performed to elucidate the behavior of the photosensitizer at the coated interface. Photoproducts were observed in parallel in the gas phase by on-line mass spectrometry and in the aqueous phase by off-line liquid chromatography coupled to high resolution mass spectrometry. Chemical mechanisms which explain the observed product distributions are proposed and discussed in detail.

## **Experimental section**

**Materials.** All chemicals were used as received, without further purification. Further details can be found in the Supplementary Information.

**UV-vis spectroscopy.** UV-vis spectra were acquired on a Cary 60 UV-Vis spectrophotometer (Agilent Technologies) using 1 cm quartz cuvettes. The absorption spectra of a 0.2 mM 4-benzoylbenzoic acid (4-BBA) aqueous solution at pH=7.0 and of neat NA were first recorded. Next, 5 mL of the 4-BBA aqueous solution was mixed with 5 mL of neat NA. The biphasic system was separated by centrifugation at 4500 rpm for 2 minutes with Fisher Bioblock Scientific Sigma centrifuge using a 15 mL Eppendorf centrifuge tube. Final UV-vis spectra of both phases were recorded separately. A similar experiment was performed without 4-BBA in the aqueous phase to check for changes in the NA spectrum due to the presence of dissolved water.

**Glancing angle laser induced fluorescence.** Fluorescence of imidazole-2-carboxaldehyde (IC) at the air-water interface has been studied by Glancing Angle Laser-Induced Fluorescence (GALIF). A detailed description of this method has been given elsewhere.<sup>21, 22</sup> Fluorescence at the air-aqueous interface was induced using the unfocussed output of a Nd:YAG-pumped Optical Parametric Oscillator (OPO) set at 285 nm, with ~ 2 mJ per 5 ns pulse. The laser beam impinged

the liquid sample surface at an angle  $>85^\circ$  from the surface normal. The fluorescence emission signal was collected using a liquid light guide suspended  $\sim 6$  mm above the impinging laser beam and transmitted through a monochromator to a photomultiplier tube. More details about experimental protocols, signal treatment and surface adsorption isotherm measurements are provided in the Supporting Information.

**Laser flash photolysis experiments.** Transient absorption experiments were carried out using the fourth harmonic (266 nm) of a Quanta Ray GCR 130-01 Nd:YAG laser, exciting the sample in a right-angle geometry with respect to the monitoring light beam. The single pulses were ca. 9 ns in duration, with an energy of  $\sim 40$  mJ/pulse. Individual cuvette samples ( $\sim 3.5$  mL volume) were used for a maximum of two consecutive laser shots in order to avoid possible substrate degradation. The transient absorption at a pre-selected wavelength was monitored by a detection system consisting of a pulsed Xenon lamp (150 W), monochromator and a photomultiplier (1P28). A spectrometer control unit was used for synchronising the pulsed light source and programmable shutters with the laser output. The signal from the photomultiplier was digitized by a programmable digital oscilloscope (HP54522A). A 32 bits RISC-processor kinetic spectrometer workstation was used to analyse the digitized signal. Stock solutions of NA and 4-BBA were prepared in Milli-Q water and mixed in an appropriate volume to obtain the desired concentrations just before each Laser Flash Photolysis (LFP) experiment. The second-order rate constant for the quenching of triplet state 4-BBA (4-BBA\*) in the presence of NA was obtained from the slope of the best-fit linear correlation between the pseudo-first-order decay constant of 4-BBA\* monitored at 540 nm vs. concentration of NA in aqueous solution. All experiments were performed at ambient temperature ( $295 \pm 2$  K) in aerated solutions.

**Quartz cell experiments – Gas phase analysis.** The experiments were performed using a 5 cm path length, 2 cm id, 14 mL cylindrical quartz cell with a gas inlet near each end (Starna, UK) 13 cm away from the output lens of a Xenon lamp (150 W Xe, LOT-QuantumDesign, France). The lamp was equipped with a 1 cm water filter in front of the reaction cell to avoid excessive heating. The cell was half-filled with 7 mL of the aqueous phase under study (pure water or an aqueous 0.1 mM 4-BBA solution) in order to maximize the surface to volume ratio ( $1.4\text{ cm}^{-1}$ ). A theoretical concentration of 2 mM of NA was achieved by the addition of 2.5  $\mu\text{L}$  of neat NA. The solution was then slightly stirred to promote NA spreading over the surface and was left to sit for 20 minutes in the dark before starting the irradiation. A gas flow at a flow rate of 200 sccm (standard cubic centimeter per minute) was continuously introduced into the cell, with 80 sccm of the outgoing gas flow sampled for analysis by a Switchable Reagent Ion-Time of Flight-Mass Spectrometer (8000 SRI-ToF-MS, Ionicon Analytik GmbH, Innsbruck, Austria). The experiments were performed either under purified compressed dry air (DF Ultrafilter, Donaldson, USA) or dry nitrogen. For the experiments performed under nitrogen, the aqueous solution was deoxygenated before NA addition by bubbling nitrogen for 25 min.

The analysis of the gas phase products was performed using both  $\text{H}_3\text{O}^+$  and  $\text{NO}^+$  ionization modes to provide information about the product functionalities.<sup>23-26</sup> Ions used for identification of functional groups in the  $\text{NO}^+$  mode are listed in Table S2 (Supporting Information). Only qualitative results and normalized signals are discussed for the  $\text{NO}^+$  reagent mode as reaction rates for most of the products with  $\text{NO}^+$  are unknown. Fragmentation patterns for the main products under our experimental conditions were carefully assessed using liquid standards diluted in 7 mL of water in the reactor and analyzed under the same conditions as the samples, as shown Table S3 (Supporting Information). Concentrations were theoretically determined from



the spectra taken in  $\text{H}_3\text{O}^+$  ionization mode, corrected for the reaction branching ratios when these were known. The global uncertainty on the absolute concentrations can be estimated to be about 40 %.<sup>27</sup> Background spectra were taken before each experiment above pure water, before adding the surfactant and an eventual photosensitizer. The error bars reported represent the standard deviation on repeated experiments ( $n \geq 2$ ). More analytical details are provided in the Supporting Information.

**Quartz cell experiments – Aqueous phase analysis.** The experiments were performed using a similar setup as for the gas phase products analysis. The cell was first filled with 11 mL of the aqueous phase under study (pure water or an aqueous 0.1 mM 4-BBA solution) and 3.8  $\mu\text{L}$  of NA was added to achieve a theoretical concentration of 2 mM. The solution was then slightly stirred to promote NA spreading over the surface and was left to sit a few minutes in the dark before a first sampling of 4 mL of the solution. The remaining 7 mL filled the cell halfway. A fixed irradiation time of 1 hour was used for all the experiments. After irradiation, the solution was stirred again for a few minutes in the dark before a second 4 mL sampling. The cell was hermetically closed during irradiation. Sampling was performed using a glass syringe through a septum before and after irradiation. The experiments were carried out either under air or under nitrogen. For the experiments performed under nitrogen, the aqueous solution was deoxygenated before NA addition by bubbling with  $\text{N}_2$  for 25 min. The empty volume of the cell was purged before hermetical closing.

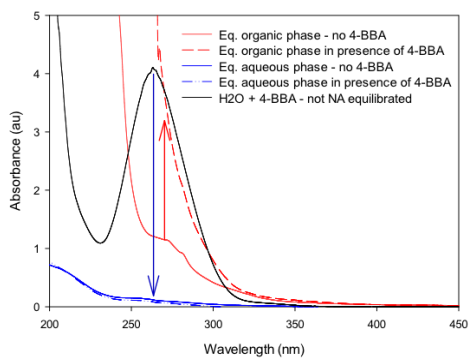
Aliquots of 500  $\mu\text{L}$  of each aqueous sample were diluted adding 500  $\mu\text{L}$  of a 1:1, v:v, water:acetonitrile mixture. Next, 200  $\mu\text{L}$  of each sample was derivatized for specific carbonyl compounds detection adding 800  $\mu\text{L}$  of a 1  $\text{mg mL}^{-1}$  PFBHA solution and leaving the obtained mixture at room temperature for 24 hours before analysis. Further details about the PFBHA

derivatization process are given in the Supporting Information. Each dilution, derivatization and analysis was performed three times. All samples were analyzed by reversed phase UltraPerformance Liquid Chromatography coupled to a Q Exactive™ High Resolution Mass Spectrometer through Heated Electrospray Ionization [UPLC/(±)HESI-HRMS, Thermo Scientific, USA]. A water/acetonitrile solvent gradient was applied. The mass spectrometer was operated in the negative ionization mode for the analysis of the non derivatized samples and in the positive ionization mode for the analysis of the derivatized ones. Reported signal intensities correspond to the total areas of the chromatographic peaks determined from the extracted ion chromatograms of the identified quasi-molecular ions. The analytical uncertainties were determined over the whole experimental period as the relative standard deviation on two series of standard injection: 8% for the non derivatized standard (negative ionization mode) and 23% for the derivatized standard (positive ionization mode). These standard deviation values are reported on the bar graphs. The standard deviation over the three replicates performed for each sample is reported only if it is above this overall experimental period standard deviation. Details about ionization conditions, calibration and data acquisition and processing are provided in the Supporting Information.

## Results and discussion

**Photosensitizer enrichment at the air-water interface.** The propensity of a photosensitizer to partition to the surface in the presence of an organic surfactant was investigated using UV-vis spectroscopy and Glancing Angle Laser Induced Fluorescence spectroscopy. Two well-known efficient photosensitizers were used, 4-benzoylbenzoic acid (4-BBA)<sup>28-30</sup> and 2-imidazole-carboxaldehyde (IC)<sup>31, 32</sup> which are both aromatics possessing a carbonyl function and therefore

200 appropriate as a proxy for CDOM.<sup>33</sup> IC, which is formed in situ in aerosols, can induce aerosol  
 201 growth<sup>31</sup> and has recently been observed in aerosol particles in the field.<sup>34</sup> Firstly, the UV-vis  
 202 absorption spectrum of an aqueous solution of 4-BBA at pH 7 was recorded, as shown in Figure  
 203 1 (black). Neat nonanoic acid was then added to this solution and aqueous and organic phases  
 204 were separated by centrifugation. The absorption spectrum of each phase was registered  
 205 separately, and displayed in Figure 1 (dashed lines). Changes in the absorption spectrum of the  
 206 two phases show an almost quantitative removal of 4-BBA from the aqueous phase. Indeed,  
 207 approximately 98% of the 4-BBA migrated from the aqueous phase into the organic phase after  
 208 seconds of contact, suggesting that the partitioning of the photosensitizer towards the organic  
 209 layer is highly favored.



210 **Figure 1.** UV-vis spectra of aqueous and NA solutions before and after equilibration with the  
 211 other phase in the presence and absence of 4-BBA. Blue and red arrows show the change in the  
 212 absorption spectra for the aqueous phase and the organic phase respectively in presence of 4-  
 213 BBA. The black line shows the absorption spectrum of an aqueous solution of 4-BBA at 0.2  
 214 mM. The red lines show the absorption spectra of the organic phase after separation of the two  
 215 phases; the solid line when no 4-BBA was present in the system, the red dashed line when in  
 216

217 presence of 4-BBA. The blue lines show the absorption spectrum of the aqueous phase after  
218 separation of the phases; the solid blue line when the system contained no 4-BBA, the blue  
219 dashed line when 4-BBA was present in the system.

220 The GALIF measurements probed the fluorescence of IC at the surface of an aqueous solution as  
221 a function of its solution concentration. The intensity of this IC surface fluorescence using pure  
222 water as a substrate was compared with the IC surface fluorescence measured at the surface of a  
223 1.5 mM solution of NA. This bulk concentration provides near-monolayer NA coverage at the  
224 air-water interface.<sup>17, 35</sup> The adsorption isotherms of IC at the aqueous-air interface, derived from  
225 these measurements and displayed in Figure 2, clearly show an enhanced fluorescence ( $\times 50$ ) in  
226 the presence of a NA coating at the surface, ~~demonstrating the propensity of the photosensitizer~~  
227 ~~to partition to the organic surface layer.~~ This difference in fluorescence can solely be attributed  
228 to changes in the surface concentration of IC demonstrating the propensity of the photosensitizer  
229 to partition to the organic surface layer, since (a) the bulk fluorescence yield of IC in nonanoic  
230 acid is lower than in pure water (Figure S1, Supporting Information) and (b) the enrichment of a  
231 compound at the surface seems to depend on its solubility in the monolayer.<sup>35</sup> This is in  
232 agreement with the results obtained by Fu et al.<sup>19</sup> that show enhanced fluorescence of IC in  
233 presence of a near monolayer of 1-octanol. Both spectroscopic techniques confirm the enhanced  
234 concentration of the photosensitizers used here at the air/water interface in the presence of an  
235 organic coating, leading very probably to an enhanced and specific photochemistry there.

Formatted: Not Highlight

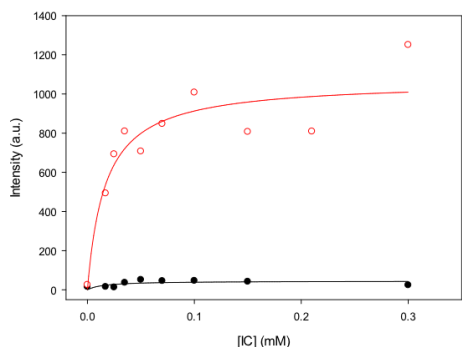


**Figure 2.** Fluorescence intensity ( $\lambda=335$  nm) of IC at the air/water interface as a function of the bulk concentration of IC, measured at a pure water surface (●) and at a nonanoic acid coated surface (○). The solid lines show the fits to Langmuir adsorption isotherms.

**Reaction rate between triplet state 4-BBA and NA.** LFP excitation of a 0.21 mM 4-BBA aqueous solution at pH 7.0 produces a transient absorption spectrum presenting two intense absorption peaks at 410 and 540 nm, illustrated in Figure S24 (Supplementary Information), which are attributed to the triplet state of 4-BBA (4-BBA\*).<sup>36</sup> The transient species decays uniformly with a pseudo-first order  $k_{540nm} = 4.76 \pm 0.11 \times 10^5 \text{ s}^{-1}$  and no residual absorbance was observed after about 5  $\mu\text{s}$ . When dissolved in neat NA the transient spectrum of 4-BBA\* presents two maxima at 350 nm and 560 nm, shown in Figure 3. After relaxation of the triplet state, approximately 2  $\mu\text{s}$  after the laser impulse, two intense bands centered at 360 nm and at 580 nm are observed. The absorption decay in this pure NA solution was followed at 560 nm and fitted well a double exponential equation, suggesting the presence of two different species. The first, short-lived species can be attributed to the excited state of 4-BBA. The second long-lived component may correspond to the ketyl radical of 4-BBA.<sup>37, 38</sup> The formation of a ketyl radical

can be explained by electron or hydrogen transfer from organic molecules (i.e. NA), a process which has previously been reported for other benzophenone derivatives.<sup>39, 40</sup>

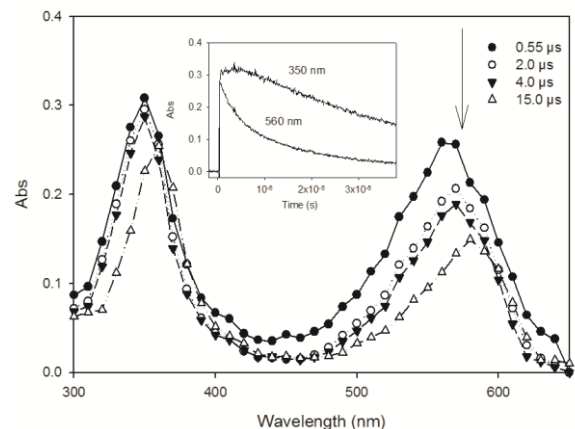


**Figure 3:** Time trend of the transient spectrum obtained upon laser-pulse excitation (266 nm, ~40 mJ) of 0.21 mM 4-BBA in NA solution. The insert shows the time trend of the signals at 350 and 560 nm

Figure S32 (Supporting Information) reports the rate constant for the pseudo-first order decay of 4-BBA\* followed at 540 nm as a function of NA concentration in an aqueous solution. The data allows for the determination of the second-order rate constant for the quenching of the triplet state by nonanoic acid  $k_{4-BBA^*,NA} = 3.0 \pm 0.5 \times 10^7 \text{ M}^{-1} \text{ s}^{-1}$ , which is competitive with rate constants reported for aliphatic carboxylic acids and hydroxyl radicals.<sup>41</sup>

**Surface microlayer photochemistry in the presence of 4-BBA.** The photo-induced chemistry occurring at the air/water interface in the presence of NA as organic coating and 4-BBA as photosensitizer was investigated. Gas-phase products were analyzed on-line while the analysis of bulk condensed phase products was performed off-line, with and without selective derivatization

of carbonyl groups. Upon irradiation, the prompt formation of gas phase products was observed (Figure S43, Supporting Information). Similarly, a wide variety of photoproducts was detected in the condensed phase after 1 h of irradiation. A complete list of the detected compounds is provided in Table S1 (Supporting Information). Nevertheless, it clearly appears that this large variety of photo-products is formed upon irradiation in the presence and in the absence of 4-BBA. The photochemistry of only NA in concentrated media, and more specifically at the air/water interface, was recently evidenced and can explain these observations.<sup>42</sup> However, here, the detection of the NA-4-BBA recombination product ( $C_{23}H_{28}O_5$ ) confirms the existence of photo-induced reactions between the photosensitizer and the organic surfactant. The ratios of the net productions for a selection of photo-products in the gas and condensed phase in the presence and in the absence of 4-BBA are displayed in Figure 4. Net production signals observed for the same series of products in both phases are shown in Figures S54 and S56 (Supporting Information).

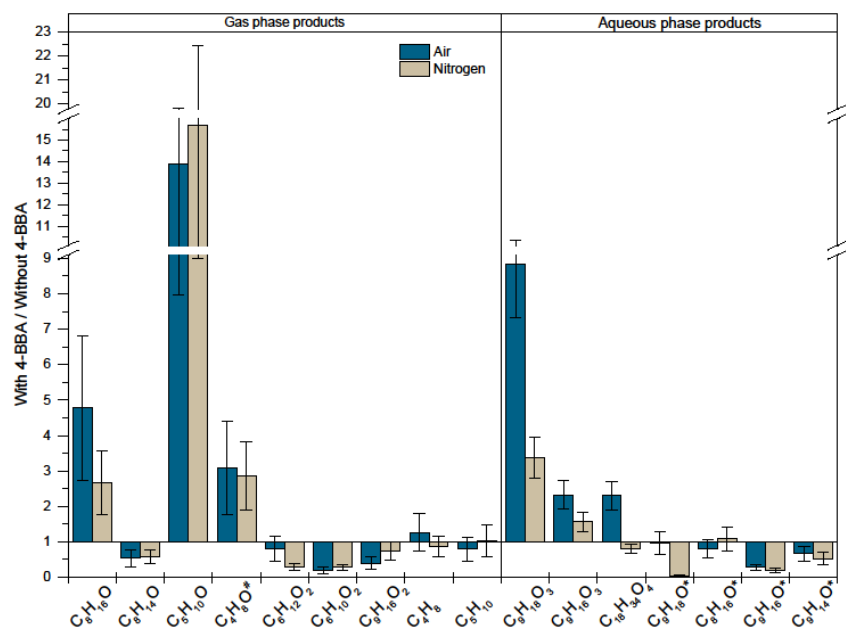


**Figure 4:** Ratio of the signal detected in the presence of 4-BBA (0.2 mM) to the signal observed without 4-BBA for a series of selected photo-products in the gas phase and in the aqueous phase, for a 2 mM NA aqueous solution. Errors reflect the analytical uncertainties (condensed phase) or repeatability between experiments (gas phase). <sup>#</sup>Identified as ketone due to NO<sup>+</sup> adduct. \*Detected as PFBHA derivatives.

Most of the observed photoproducts were oxygenated. Octanal (C<sub>8</sub>H<sub>16</sub>O) was one of the main products in both phases. Aldehydes and ketones (< C<sub>9</sub>), including unsaturated and dicarbonyl compounds, were also detected. Octenal (C<sub>8</sub>H<sub>14</sub>O) was one of the main unsaturated oxygenated compounds observed. In the condensed phase, C<sub>9</sub> products with three or more oxygen atoms, such as C<sub>9</sub>H<sub>18</sub>O<sub>3</sub> and C<sub>9</sub>H<sub>16</sub>O<sub>3</sub>, were also detected. These compounds can be tentatively identified



as NA bearing additional hydroxyl and/or carbonyl functions. They were not detected in the gas phase, probably due to their low volatility. Small acids ( $< C_9$ ) were detected in both phases but only in rather low abundances. Some unsaturated acids were observed as well, the main one being  $C_9H_{16}O_2$ , identified as nonenoic acid. Alkenes could not be evidenced in the condensed phase due to the electrospray ionization limitation for non-polar compounds, but  $C_4H_8$  and  $C_5H_{10}$  were the most abundant unsaturated products detected in the gas phase. Additionally, compounds bearing more than nine carbon atoms were observed in the condensed phase, such as  $C_{18}H_{34}O_4$ ,  $C_{28}H_{22}O_6$  and  $C_{23}H_{28}O_5$ . These molecular formulae can be attributed to the dimer of NA, the dimer of 4-BBA and, as already mentioned, the combination of NA and 4-BBA, respectively. Experiments performed using IC as the photosensitizer showed overall a very similar pattern of product formation, but with lower intensities for the products, probably due to the lower quantum yield of the triplet state of IC compared to 4-BBA. Figure S76, Supporting Information displays details of these results.

Interestingly, the formation of certain products is favored in the presence of 4-BBA while the formation of others is hindered, as shown in Figure 4. Enhanced production is observed in the presence of 4-BBA for some oxidized and saturated compounds, such as the  $C < 9$  aldehydes ( $C_8H_{16}O$ ,  $C_5H_{10}O$ ,  $C_4H_8O$ ) and various  $C_9$  oxidation products ( $C_9H_{18}O_3$  and  $C_9H_{16}O_3$ ). Photo-products hindered in the presence of 4-BBA are the  $C_9$  carbonyls, nonanal and nonenal, and in a more general way the compounds presenting a C-C double bond. Very similar observations arose from experiments performed in the presence and in the absence of  $H_2O_2$  as photo-initiator, as can be seen in Figure S87 (Supporting Information),<sup>42</sup> hydroxyl radicals being also able to react quickly with C-C double bonds [leading to functionalization and fragmentation](#)<sup>43</sup>. Competition for H abstraction between 4-BBA\* and NA\* could contribute to the fact that saturated and

unsaturated C<sub>9</sub> aldehydes, expected to be specific to the reactivity of NA alone photochemistry in concentrated media, are hindered in the presence of 4-BBA.<sup>42</sup> Triplet state 4-BBA can react with organics such as NA through H-abstraction, to initiate radical chemistry,<sup>44, 45</sup> a pathway supported by the similarity between the series of products observed in these experiments with those obtained using H<sub>2</sub>O<sub>2</sub> as photo-initiator.<sup>42</sup> The hydroxyl radical generated by H<sub>2</sub>O<sub>2</sub> photolysis upon irradiation is expected to react with NA only via H-abstraction. Recently Rossignol et al.<sup>42</sup> have demonstrated that radical-initiated photochemistry of aqueous solutions containing only NA readily occurs, and suggested that this is initiated by the formation of an NA excited state, followed either by H-abstraction from another NA molecule or by a homolytic cleavage releasing a hydroxyl radical. If this hypothesis is true, the formation of C<sub>9</sub> aldehydes would be specific to the photochemistry of NA alone, as these compounds are formed directly from the excited state of NA. The results detailed here suggest that in the presence of 4-BBA (or H<sub>2</sub>O<sub>2</sub>), a competition between the photochemistry of NA-only chemistry and “traditional” H-abstraction by an excited photosensitizer occurs, with the products derived from the NA radical formed after H-abstraction on the carbon chain being favored, and those derived directly from the NA excited state hindered.

In order to investigate the role of oxygen in this chemistry, all the experiments were repeated under nitrogen using deoxygenated solutions. The net production of the same selection of compounds under these two conditions is compared Figures S54 and S65 (Supporting Information) and Figure 4 compares the ratios of the signals obtained under these two conditions. The highly oxygenated C<sub>9</sub> products are clearly favored when oxygen is more abundant (e.g. C<sub>9</sub>H<sub>18</sub>O<sub>3</sub> and C<sub>9</sub>H<sub>16</sub>O<sub>3</sub>). While on the other hand, the dimers (e.g. C<sub>18</sub>H<sub>34</sub>O<sub>4</sub>) as well as the unsaturated C<sub>9</sub> acid (C<sub>9</sub>H<sub>16</sub>O<sub>2</sub>) appear to be favored in an oxygen-poor environment. The

formation of alkenes also seems to be favored under nitrogen. The influence of oxygen is less clear for the carbonyl compounds and in particular for those bearing an unsaturation, as illustrated for octenal.

From these observations a general mechanism of the photosensitized degradation of NA may be derived; this is given in Figure 5. After the initial H-abstraction by the excited state of the photosensitizer, two pathways are expected: the addition of molecular oxygen or radical-radical reactions. The latter explains the formation of NA dimers, but also the formation of the observed NA-4-BBA and 4-BBA-4-BBA recombination products. This type of fast radical recombination, has been observed previously in photosensitized reactions in aerosols,<sup>31</sup> but occurs only where high radical concentrations are achieved.<sup>46</sup> The presence of such recombination products thus highlights some particular features of the enhanced concentration at the air/water interface. This surface enhanced concentration can also favor radical-radical disproportionation reactions,<sup>19</sup> explaining the formation of nonenoic acid and possibly of other unsaturated compounds. Molecular oxygen addition is not expected to be specific to the interface, as oxygen readily dissolves in bulk water, where similar chemistry, leading to the formation of a peroxy radical, has been reported.<sup>47</sup> This peroxy radical is then expected either to fragment, leading to the formation of octanal, or to evolve toward hydroxyl or carbonyl functions. These products can then undergo similar processes as the initial NA molecules, leading to the formation of second generation products. The competition between radical-radical reactions promoted at the interface and oxygen addition appears thus to play a key role in the distribution of the products. This is highlighted by the fact that recombination and disproportionation products were observed to be favored in an oxygen-poor environment. Considering the proposed mechanism, the formation of unsaturated aldehydes, apparently not impacted by the presence of oxygen, also underlines this

361 competition; while oxygen is required to form the saturated aldehyde on which H-abstraction can  
362 then occur, disproportionation reactions leading to the unsaturated aldehyde is favored under  
363 nitrogen.

364 Alkenes, which are not mentioned on the proposed mechanism, could arise from the photolytic  
365 cleavage of the carbonyl compounds, but this does not strictly match the observations, as the  
366 formation of the main alkenes observed, butene and pentene, appears to be favored under  
367 nitrogen (Figure S54, Supporting Information). Another pathway could invoke the cyclization of  
368 the NA radical leading to the formation of a C<sub>5</sub> or C<sub>4</sub> lactone and a related C<sub>4</sub> or C<sub>5</sub> alkyl radical  
369 fragment, which ultimately gives rise to butene and pentene (Figure S98, Supporting  
370 Information). This mechanism is in agreement with the observation that these products are  
371 favored under nitrogen since the cyclization and disproportionation steps would both be in  
372 competition with oxygen addition.

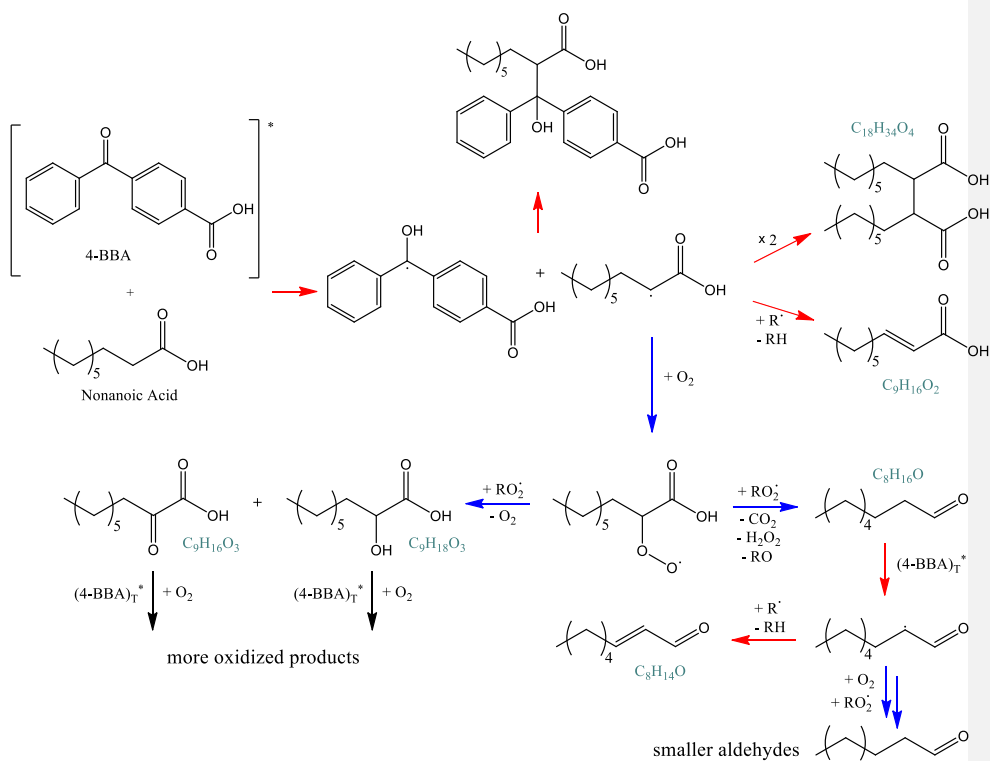


**Figure 5.** Proposed mechanism for the photosensitized degradation of NA. Blue highlighted pathways are expected to be promoted under air and red highlighted pathways at the interface and under nitrogen. The products identified by their chemical formulas (grey) correspond to products shown in Figure 4.

In conclusion, this study relates the photochemical production of functionalized and unsaturated compounds at an air/water interface in the presence of a carboxylic acid, nonanoic acid, as surfactant. When a photosensitizer, such as 4-BBA or IC, is present in the aqueous solution, it will rapidly partition to the organic surface layer where it can induce radical reactions

through a hydrogen abstraction on a NA molecule, leading to the formation of a large variety of compounds.

The photochemical production and the gas phase release of such unsaturated and functionalized compounds will influence the oxidative capacity of the atmosphere and can lead to secondary aerosol formation. This interfacial photochemistry has potentially a very large impact, especially as both reactants, the photosensitizer and the substrate can be naturally present at high concentrations at the surface, providing a very favorable venue for this new type of photochemistry. Although the photochemistry triggered by the photosensitizer competes with the photochemistry induced by a carboxylic acid at the surface layer, it is generally leading more efficiently to oxidized products. Moreover, this photochemistry seems to occur with different types of photosensitizers (4-BBA, IC, H<sub>2</sub>O<sub>2</sub>) and surfactant organic coatings (nonanoic acid, octanol, heptanol), meaning that these photosensitized processes could be much more generally occurring than previously thought. We expect that this chemistry will apply especially to ocean surfaces, cloud droplets and evanescent atmospheric droplets, where organics are expected to be enriched at the air interface.

#### ASSOCIATED CONTENT

**Supporting Information.** Experimental setup details, Tables S1-3 and Figures S1-98. This material is available free of charge via the Internet at <http://pubs.acs.org>.

#### AUTHOR INFORMATION

##### Corresponding Author

404 Christian GEORGE

405 E-mail: christian.george@ircelyon.univ-lyon1.fr

406 Phone number: (33) (0)4 37 44 54 92

407 Fax number: (33) (0)4 72 44 84 38

408 ~~\* E-mail: christian.george@ircelyon.univ-lyon1.fr. Phone: (33) (0)4 72 44 54 92~~

409 #These authors contributed equally.

#### 410 **Funding Sources**

411 This study was supported by the European Research Council under the European Union's  
412 Seventh Framework Program (FP/2007-2013) / ERC Grant Agreement 290852 – AIRSEA and  
413 by the Marie Curie International Research Staff Exchange project AMIS (Grant 295132). The  
414 GALIF experiments were supported by a grant from NSERC (Canada).

#### 415 **Notes**

416 The authors declare no competing financial interest.

#### 417 **ACKNOWLEDGMENT**

418 This study was supported by the European Research Council under the European Union's  
419 Seventh Framework Program (FP/2007-2013) / ERC Grant Agreement 290852 – AIRSEA and  
420 by the Marie Curie International Research Staff Exchange project AMIS (Grant 295132). DJD  
421 thanks NSERC for continuing financial support.

422

## 423 REFERENCES

- 424 1. Donaldson, D. J.; Vaida, V., The influence of organic films at the air-aqueous boundary  
425 on atmospheric processes. *Chem. Rev.* **2006**, *106*, (4), 1445-1461.
- 426 2. Zhou, S.; Gonzalez, L.; Leithead, A.; Finewax, Z.; Thalman, R.; Vlasenko, A.; Vagle, S.;  
427 Miller, L. A.; Li, S. M.; Bureekul, S.; Furutani, H.; Uematsu, M.; Volkamer, R.; Abbatt, J.,  
428 Formation of gas-phase carbonyls from heterogeneous oxidation of polyunsaturated fatty acids at  
429 the air-water interface and of the sea surface microlayer. *Atmos. Chem. Phys.* **2014**, *14*, (3),  
430 1371-1384.
- 431 3. Liss, P. S.; Duce, R. A., *The sea surface and global change*. 2005.
- 432 4. Phillips, S. M.; Smith, G. D., Light Absorption by Charge Transfer Complexes in Brown  
433 Carbon Aerosols. *Environmental Science & Technology Letters*, **2014**, *1*, (10), 382-386.
- 434 5. Carlson, D. J., Dissolved organic materials in surface microlayers - temporal and spatial  
435 variability and relation to sea state. *Limnol. Oceanogr.* **1983**, *28*, (3), 415-431.
- 436 6. Carlson, D. J.; Mayer, L. M., Enrichment of dissolved phenolic material in the surface  
437 microlayer of coastal waters. *Nature* **1980**, *286*, (5772), 482-483.
- 438 7. Donaldson, D. J.; George, C., Sea-surface chemistry and its impact on the marine  
439 boundary layer. *Environ. Sci. Technol.* **2012**, *46*, (19), 10385-10389.
- 440 8. Ehrhardt, M. G.; Weber, R. R., Sensitized photooxidation of methylcyclohexane as a  
441 thin-film on seawater by irradiation with natural sunlight. *Fresenius J. Anal. Chem.* **1995**, *352*,  
442 (3-4), 357-363.
- 443 9. Wurl, O.; Wurl, E.; Miller, L.; Johnson, K.; Vagle, S., Formation and global distribution  
444 of sea-surface microlayers. *Biogeosciences* **2011**, *8*, (1), 121-135.
- 445 10. Cunliffe, M.; Engel, A.; Frka, S.; Gase, A.; Japarovic, A.; B.-e.; Guitart, C.; Murrell, J. C.;  
446 Salter, M.; Stolle, C.; Upstill-Goddard, R.; Wurl, O., Sea surface microlayers: A unified  
447 physicochemical and biological perspective of the air-sea-ocean interface. *Progress in*  
448 *Oceanography-Oceanogr.* **2013**, *109*, (0), 104-116.
- 449 11. Carpenter, L. J.; Nightingale, P. D., Chemistry and release of gases from the surface  
450 ocean. *Chem. Rev.* **2015**, *115*, (10), 4015-4034.
- 451 12. Reeser, D. I.; Jammoul, A.; Clifford, D.; Brigante, M.; D'Anna, B.; George, C.;  
452 Donaldson, D. J., Photoenhanced reaction of ozone with chlorophyll at the seawater surface. *J.*  
453 *Phys. Chem. C* **2008**, *113*, (6), 2071-2077.
- 454 13. Stemmler, K.; Ammann, M.; Donders, C.; Kleffmann, J.; George, C., Photosensitized  
455 reduction of nitrogen dioxide on humic acid as a source of nitrous acid. *Nature* **2006**, *440*,  
456 (7081), 195-198.
- 457 14. Jammoul, A.; Dumas, S.; D'Anna, B.; George, C., Photoinduced oxidation of sea salt  
458 halides by aromatic ketones: A source of halogenated radicals. *Atmos. Chem. Phys.* **2009**, *9*, (13),  
459 4229-4237.
- 460 15. Reeser, D. I.; George, C.; Donaldson, D. J., Photooxidation of Halides by Chlorophyll at  
461 the Air-Salt Water Interface. *Journal of Physical-Phys. Chemistry-Chem. A* **2009**, *113*, (30),  
462 8591-8595.
- 463 16. Gever, J. R.; Mabury, S. A.; Crosby, D. G., Rice field surface microlayers: Collection,  
464 composition and pesticide enrichment. *Environ. Toxicol. Chem.* **1996**, *15*, (10), 1676-1682.



17. Ciuraru, R.; Fine, L.; van Pinxteren, M.; D'Anna, B.; Herrmann, H.; George, C., Photosensitized production of functionalized and unsaturated organic compounds at the air-sea interface. *Sci. Rep.* **2015**, *5*, 12741.
18. Ciuraru, R.; Fine, L.; van Pinxteren, M.; D'Anna, B.; Herrmann, H.; George, C., Unravelling new processes at interfaces: Photochemical isoprene production at the sea surface. *Environ. Sci. Technol.* **2015**, *49*, (22), 13199-13205.
19. Fu, H.; Ciuraru, R.; Dupart, Y.; Passananti, M.; Tinel, L.; Rossignol, S.; Perrier, S.; Donaldson, D. J.; Chen, J.; George, C., Photosensitized production of atmospherically reactive organic compounds at the air/aqueous interface. *J. Am. Chem. Soc.* **2015**, *137*, (26), 8348-8351.
20. Chebbi, A.; Carlier, P., Carboxylic acids in the troposphere, occurrence, sources, and sinks: A review. *Atmospheric Atmos. Environment Environ.* **1996**, *30*, (24), 4233-4249.
21. Mmereki, B. T.; Donaldson, D. J., Laser induced fluorescence of pyrene at an organic coated air-water interface. *Phys. Chem. Chem. Phys.* **2002**, *4*, (17), 4186-4191.
22. Mmereki, B. T.; Donaldson, D. J., Direct observation of the kinetics of an atmospherically important reaction at the air-aqueous interface. *Journal-J. of Physical Phys. Chemistry Chem. A* **2003**, *107*, (50), 11038-11042.
23. Jordan, A.; Haidacher, S.; Hanel, G.; Hartungen, E.; Herbig, J.; Maerk, L.; Schottkowsky, R.; Seehauser, H.; Sulzer, P.; Maerk, T. D., An online ultra-high sensitivity Proton-transfer-reaction mass-spectrometer combined with switchable reagent ion capability (PTR+SRI-MS). *Int. J. Mass Spectrom.* **2009**, *286*, (1), 32-38.
24. Karl, T.; Hansel, A.; Cappellin, L.; Kaser, L.; Herdinger-Blatt, I.; Jud, W., Selective measurements of isoprene and 2-methyl-3-buten-2-ol based on NO<sup>+</sup> ionization mass spectrometry. *Atmos. Chem. Phys.* **2012**, *12*, (24), 11877-11884.
25. Knighton, W. B.; Fortner, E. C.; Herndon, S. C.; Wood, E. C.; Miake-Lye, R. C., Adaptation of a proton transfer reaction mass spectrometer instrument to employ NO<sup>+</sup> as reagent ion for the detection of 1,3-butadiene in the ambient atmosphere. *Rapid Commun. Mass Spectrom.* **2009**, *23*, (20), 3301-3308.
26. Smith, D.; Spanel, P., Selected ion flow tube mass spectrometry (SIFT-MS) for on-line trace gas analysis. *Mass Spectrometry Spectrom. Reviews Rev.* **2005**, *24*, (5), 661-700.
27. Herndon, S. C.; Rogers, T.; Dunlea, E. J.; Jayne, J. T.; Miake-Lye, R.; Knighton, B., Hydrocarbon emissions from in-use commercial aircraft during airport operations. *Environ. Sci. Technol.* **2006**, *40*, (14), 4406-4413.
28. Monge, M. E.; Rosenørn, T.; Favez, O.; Müller, M.; Adler, G.; Abo Riziq, A.; Rudich, Y.; Herrmann, H.; George, C.; D'Anna, B., Alternative pathway for atmospheric particles growth. *Proc. Natl. Acad. Sci.* **2012**, *109*, (18), 6840-6844.
29. Net, S.; Nieto-Gligorovski, L.; Gligorovski, S.; Temime-Roussel, B.; Barbati, S.; Lazarou, Y. G.; Wortham, H., Heterogeneous light-induced ozone processing on the organic coatings in the atmosphere. *Atmospheric Atmos. Environment Environ.* **2009**, *43*, (9), 1683-1692.
30. Net, S.; Nieto-Gligorovski, L.; Gligorovski, S.; Wortham, H., Heterogeneous ozonation kinetics of 4-phenoxyphenol in the presence of photosensitizer. *Atmos. Chem. Phys.* **2010**, *10*, (4), 1545-1554.
31. Rossignol, S.; Aregahegn, K. Z.; Tinel, L.; Fine, L.; Nozière, B.; George, C., Glyoxal induced atmospheric photosensitized chemistry leading to organic aerosol growth. *Environ. Sci. Technol.* **2014**, *48*, (6), 3218-3227.

32. Tinel, L.; Dumas, S.; George, C., A time resolved study of the multiphase chemistry of excited carbonyls: Imidazole-2-carboxaldehyde and halides. *C. R. Chim.* **2013**, *17*, (7-8), 801-807.
33. Canonica, S.; Jans, U.; Stemmler, K.; Hoigne, J., Transformation kinetics of phenols in water: Photosensitization by dissolved natural organic material and aromatic ketones. *Environ. Sci. Technol.* **1995**, *29*, (7), 1822-1831.
34. Teich, M.; van Pinxteren, D.; Kecorius, S.; Wang, Z.; Herrmann, H., First quantification of imidazoles in ambient aerosol particles: Potential photosensitizers, brown carbon constituents, and hazardous components. *Environ. Sci. Technol.* **2016**, *50*, (3), 1166-1173.
35. Mmereki, B. T.; Donaldson, D. J.; Gilman, J. B.; Eliason, T. L.; Vaida, V., Kinetics and products of the reaction of gas-phase ozone with anthracene adsorbed at the air-aqueous interface. *Atmospheric Atmos. Environment Environ.* **2004**, *38*, (36), 6091-6103.
36. Hurley, J. K.; Linschitz, H.; Treinin, A., Interaction of halide and pseudohalide ions with triplet benzophenone-4-carboxylate: Kinetic and radical yields. *J. Phys. Chem.* **1988**, *92*, (18), 5151-5159.
37. Bhasikuttan, A. C.; Singh, A. K.; Palit, D. K.; Sapre, A. V.; Mittal, J. P., Laser flash photolysis studies on the monohydroxy derivatives of benzophenone. *J. Phys. Chem. A* **1998**, *102*, (20), 3470-3480.
38. Sul'timova, N. B.; Levin, P. P.; Chaikovskaya, O. N., Laser photolysis study of the transient products of 4-carboxybenzophenone-sensitized photolysis of chlorophenoxyacetic acid-based herbicides in aqueous micellar solutions. *High Energ. Chem.* **2010**, *44*, (5), 393-398.
39. Barsotti, F.; Brigante, M.; Sarakha, M.; Maurino, V.; Minero, C.; Vione, D., Photochemical processes induced by the irradiation of 4-hydroxybenzophenone in different solvents. *Photochem. Photobiol. Sci.* **2015**, *14*, (11), 2087-2096.
40. Woodward, J. R.; Sakaguchi, Y., Radical pair kinetics in the hydrogen abstraction of benzophenone derivatives in micellar solutions, studied by pulsed microwave irradiation. *J. Phys. Chem. A* **2001**, *105*, (16), 4010-4018.
41. Buxton, G. V.; Greenstock, C. L.; Helman, W. P.; Ross, A. B., Critical-review of rate constants for reactions of hydrated electrons, hydrogen-atoms and hydroxyl radicals (.OH/.O-) in aqueous-solution. *Journal-J. of Physical-Phys. and Chemical-Chem. Reference-Ref. Data* **1988**, *17*, (2), 513-886.
42. Rossignol, S.; Tinel, L.; Bianco, A.; Passananti, M.; Brigante, M.; Donaldson, D. J.; George, C., Atmospheric photochemistry at a fatty acid coated air/water interface. *Science* **2016**, *353*, (6300), 699-702. *in press*.
43. Kroll, J. H.; Smith, J. D.; Che, D. L.; Kessler, S. H.; Worsnop, D. R.; Wilson, K. R., Measurement of fragmentation and functionalization pathways in the heterogeneous oxidation of oxidized organic aerosol. *Phys. Chem. Chem. Phys.* **2009**, *11*, (36), 8005-8014.
44. Foote, C. S., Mechanisms of photosensitized oxidation. *Science* **1968**, *162*, (3857), 963-970.
45. Foote, C. S., Definition of type-I and type-II photosensitized oxidation. *Photochemistry Photochem. and Photobiology Photobiol.* **1991**, *54*, (5), 659-659.
46. Parsons, A., *An introduction to free radical chemistry*. Wiley-Blackwell Cambridge, 1996; p 238.

Formatted: Font: Not Bold

Formatted: Font: Not Bold, Italic

Formatted: Font: Not Bold

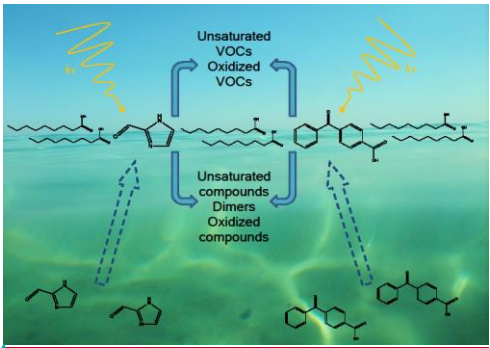
Formatted: Font: Not Bold, Italic

Formatted: Font: Not Bold

552 47. von Sonntag, C.; Schuchmann, H.-P., The Elucidation of peroxy radical reactions in  
553 aqueous solution with the help of radiation-chemical methods. *Angew. Chem. Int. Ed.* **1991**, *30*,  
554 (10), 1229-1253.

555  
556  
557

558 TOC/Graphical abstract:



Field Code Changed

559